HHSF223201610542P
Final Report May 22, 2017

Lark L. Coffey[1], Koen Van Rompay[1], Rebekah Keesler[1], Patricia Pesavento[1], Anil Singapuri[1], Jeff Linnen[2] and Kui Gao[2]
[1]University of California, Davis, California, [2]Hologic, San Diego, California,

Project Title: Companion Studies to Define the Distribution and Duration of Zika virus Infection in Non-Human Primates

Project Goal: Define the distribution and duration of Zika virus in various tissues of pregnant rhesus macaques pregnant rhesus macaques

Synopsis: The FDA and University of California, Davis partnered to elucidate which tissues Zika virus targets in non-human primates. Information from these studies will inform safety policies related to organs and tissues by increasing understanding of the risk of Zika virus transmission through infected tissue products and ultimately improving product safety.

Abstract
Background: To better understand the risk of potential for transmission of Zika virus in tissues and organs, this study investigates ZIKV tissue tropism using a nonhuman primate model. For example, prolonged persistence of ZIKV has been observed in tissues such as placenta and semen. However, the presence and persistence of ZIKV, and therefore its potential for transmission, in other tissues are largely unknown.

Methodology: For this study, reverse transcription polymerase chain reaction (RT-PCR) was used to detect and quantify levels of ZIKV RNA in 38 different tissues from 4 pregnant rhesus macaques inoculated intravenously with a Brazilian strain of ZIKV during the 1st or 2nd trimester and euthanized near the end of gestation, except in 1 animal whose fetus died 7 days post-inoculation (dpi). Tissues with detectable ZIKV RNA were titrated by plaque assay to detect infectious ZIKV. Tissue sections were also examined for histopathological lesions and probed by *in situ* hybridization to localize ZIKV RNA.

Results: ZIKV RNA was detected in selected tissues from pregnant macaques 7, 65, 87, or 105 dpi. The animal sampled 7 dpi had the highest rate of ZIKV RNA positive tissues (with levels up to 8.8 $\log_{10}$ RNA copies/gram tissue), while the other 3 animals had fewer positive tissues with lower ZIKV RNA levels (up to 6.4 $\log_{10}$ genome copies/gram tissue). Lymphatic and genitourinary tract tissues were primary reservoirs, as evidenced by ZIKV RNA in all four animals. Some macaques also contained detectable ZIKV RNA in skin, cardiopulmonary, musculoskeletal, and digestive tract tissues. Despite the presence of ZIKV RNA in many tissues, infectious ZIKV was only detected via plaque assay in placenta tissues from 3 animals and in the umbilical cord and amniotic fluid from the animal sampled 7 dpi. Histopathologic changes were not remarkable except in the placenta of the animal sampled 7 dpi but *in situ* hybridization detection of ZIKV RNA in tissues confirmed and refined the RT-PCR findings, with viral RNA present in cells of the lymphatic, genitourinary, and digestive tract tissues, with most RNA in lymph node germinal centers of dams euthanized 65-87 dpi.

Conclusions: The results from this study reveal that ZIKV RNA is detectable in macaque tissues for more than 3 months after inoculation, the longest time post-inoculation that animals in this study were followed. Infectious virus was also detected in placental tissues and the umbilical cord for more than 3 months. These data indicate that ZIKV can persist in macaque tissues for periods beyond acute viremia.

Introduction

Zika virus is a globally emerging human pathogen. Mosquito-borne Zika virus (ZIKV, family *Flaviviridae*, genus *Flavivirus*) was declared a 'public health emergency' by the World Health Organization in February 2016. The rapid and explosive spread of ZIKV in 60 new countries and territories in the Americas and Asia since June 2015 has caused millions of infections worldwide and nearly 20,000 cases in US territories as of September 2016 (1). ZIKV has now also been identified as a cause of fetal microcephaly and death (2). Since it was first isolated in 1947 in the Zika forest in Uganda, ZIKV periodically emerged from its forest monkey-mosquito-monkey cycle to cause focal human epidemics. The recent devastating epidemics since 2013 in French Polynesia, Brazil, and now most countries and territories in South and Central America, resulted from viral adaptation to an exclusive human-mosquito-human cycle. As of March 2017, ZIKV has expanded to establish local transmission in South Florida, causing more than 200 confirmed cases, and in South Texas where 6 local cases were reported (1), indicating the establishment of an autochthonous cycle in the continental US. Viral genomes from the ongoing American epidemic, including those isolated from a 2013 outbreak in French Polynesia, cluster genetically with Asian lineage ZIKV strains suggesting a single introduction of the virus into the Americas (3), and highlighting how international travel can seed global spread from endemic transmission foci (4). The rapid colonization of the Americas by ZIKV in only ≈1 year suggests that even more ZIKV outbreaks will likely occur in new areas in the future, especially if introduced into flavivirus-naïve populations, and possibly mediated by herd immunity to dengue virus that may enhance ZIKV infection to produce more severe disease (5-7). Given the overlapping presence of both primary ZIKV vectors, *Aedes aegypti* and *Aedes albopictus,* within major human population centers (8), coupled with the risk for sexual transmission, ZIKV has the potential to spread outside of Florida and to become established throughout the southern US. In the absence of a licensed vaccine, mosquito control remains the only public health intervention response to prevent infections. However, vector control programs have done little to eliminate the primary vectors from urban areas or to prevent epidemic spread in the Neotropics or Asia.

Zika virus tropism and persistence is unknown. Prolonged persistence of ZIKV has now been observed in placentas and semen (9-11). While a recent report of ZIKV infection in kidney and liver transplant recipients describes complications with full recovery is reassuring, the effects of ZIKV in immune suppressed solid organ transplant recipients is still unknown (10). The presence and persistence of ZIKV in other tissues are largely unknown and it is important to understand given the potential for organ and tissue transplant transmission.

Rhesus macaque model development at the UC Davis California National Primate Research Center. The availability of a primate model of ZIKV infection is extremely timely and useful for understanding human ZIKV infection dynamics and disease. We performed pilot studies in rhesus macaques that better model human ZIKV than mice due to more similar placental and neurologic development (12, 13). Upon further refinement, this animal model will become a highly valuable resource to investigate the various aspects of pathogenesis and to test intervention strategies, including vaccines or other therapeutics, as well as strategies to interrupt transfusion, tissue or organ transmission to protect the human tissue, organ, and blood supply. Such studies can guide clinical trials with the ultimate goal of mitigating the ZIKV pandemic. Given that the frequency and timing of transplacental ZIKV transmission in humans is uncertain and likely variable, our pilot studies ensured fetal macaque infection by bypassing the transplacental barrier through combined intravenous (IV) maternal and intra-amniotic (IA) fetal ZIKV inoculation at defined gestational times. This FDA contract capitalizes on the samples collected in this pilot study to investigate tissue targets of ZIKV.

Methods

Animals, care, use, and sample collection

The 4 dams in this study were healthy adult 6 to 14 years old female Indian-origin rhesus macaques (*Macaca mulatta*) that had all had prior infants and were Mamu-A*01 negative, from the type D retrovirus-free, SIV-free and simian lymphocyte tropic virus type 1-free colony. All dams were confirmed to be antibody negative for West Nile virus (WNV) using a simian WNV ELISA (Xpress Bio). Animals were not screened for dengue virus antibody given the absence of local circulation in California. All subjects were housed and all experimental procedures were performed at the California National Primate Research Center (CNPRC), a facility accredited by the Association for Assessment and Accreditation of Laboratory Animal Care International (AAALAC). All animal care was performed in compliance with the Guide for the Care and Use of Laboratory Animals provided by the Institute for Laboratory Animal Research (2011). The macaques were housed indoor in stainless steel cages (Lab Product, Inc.) and were exposed to a 12 hour light/dark cycle, 65-75°F, and 30-70% room humidity. Animals had free access to water and received commercial chow (high protein diet, Ralston Purina Co.) and fresh fruit supplements. The study was approved by the Institutional Animal Care and Use Committee of the University of California, Davis. When necessary, macaques were immobilized with ketamine HCl (Parke-Davis) at approximately 10 mg/kg and injected intramuscularly after overnight fasting. Blood samples were collected using venipuncture. Cerebrospinal fluid was collected via a cervical spinal tap. Urine was collected on days of sedation via cystocentesis or from the cage pan. Amniocentesis was conducted via ultrasound guidance. Since frequent anesthesia and amniocentesis are risk factors for pregnancy loss, we also treated 3 non-infected pregnant macaques on the same schedule with frequent manipulations as ZIKV-inoculated animals; all had normal fetal development. Animals were euthanized with an overdose of pentobarbital, followed by necropsy with extensive tissue collection.

ZIKV inoculations

Zika virus (strain Zika virus/H.sapiens-tc/BRA/2015/Brazil_SPH2015; Genbank Accession number KU321639.1) isolated from the plasma of a human in Brazil in 2015 was passaged once on Vero cells and then titrated by Vero cell plaque assay. The inoculum was adjusted to 5.0 $\log_{10}$ PFU (corresponding to 7.8 $\log_{10}$ RNA) in 1 ml of RPMI-1640 medium and injected both intravenously in the saphenous vein of the 4 dams and via ultrasound-guided intra-amniotic inoculation. Ultrasound was used to determine gestational age of dams that had been bred. To reflect first and second trimester infections, where the macaque gestational period is approximately 165 days, one animal each at 41, 50, 64 and 90 gestation days (GD) was inoculated. Inocula were back-titrated by plaque assay to verify the administered dose. The inoculum tested negative for mycoplasma contamination by deep sequencing (not shown).

Selection, collection and preservation of tissues for analyses

Table 1: List of macaque tissue samples for Zika virus testing	
1. Dura Mater	2. Pericardium
3. Liver	4. Kidney
5. Eye cornea, left	6. Skin, shaved, dermis and epidermis, intrascapular
7. Eye sclera, left	8. Skin, shaved, dermis and epidermis, medial thigh
9. Inguinal lymph node	10. Muscle, quadriceps
11. Bone marrow	12. Cartilage, left knee
13. Cervical lymph node	14. Tendon/ligaments, left knee
15. Retropharyngeal lymph node	16. Bone (femur)
17. Oropharynx	18. Finger, distal 2 cm
19. Lung, caudal	20. Fascia

21. Bronchi	22. Fat
23. Bronchial lymph nodes	24. Ovary
25. Pancreas	26. Placenta
27. Duodenum	28. Umbilical cord blood
29. Jejunum	30. Amniotic fluid
31. Ileum	32. Umbilical cord
33. Aortic valve	34. Peri-aortic lymph ode
35. Aorta, thorax	36. Pulmonary artery, left and right
37. Aorta, abdomen	38. Heart left and right, atrioventricular-valves

The tissues in Table 1 were subjected to testing. At necropsy, solid tissues were processed into tubes and then flash frozen on dry ice before transfer to -80°C prior to testing to allow for viral RNA (vRNA) or infectious virus detection. Solid tissues from tissue sections adjacent to those collected into tubes were placed in tissue cassettes in 10% formalin for histopathologic and *in situ* hybridization (ISH) analyses.

Workflow for analyzing tissues

Zika virus RNA levels were first measured by qRT-PCR in tissues (step 1 in Figure 1), followed by re-testing by the more sensitive Hologic Aptima® assay (step 2). Tissues that tested vRNA positive by either assay were then titrated for infectious virus (step 3) and examined histologically for pathologic changes as well as by ZIKV-RNA specific in situ hybridization (step 4) to localize vRNA in cells within tissues.

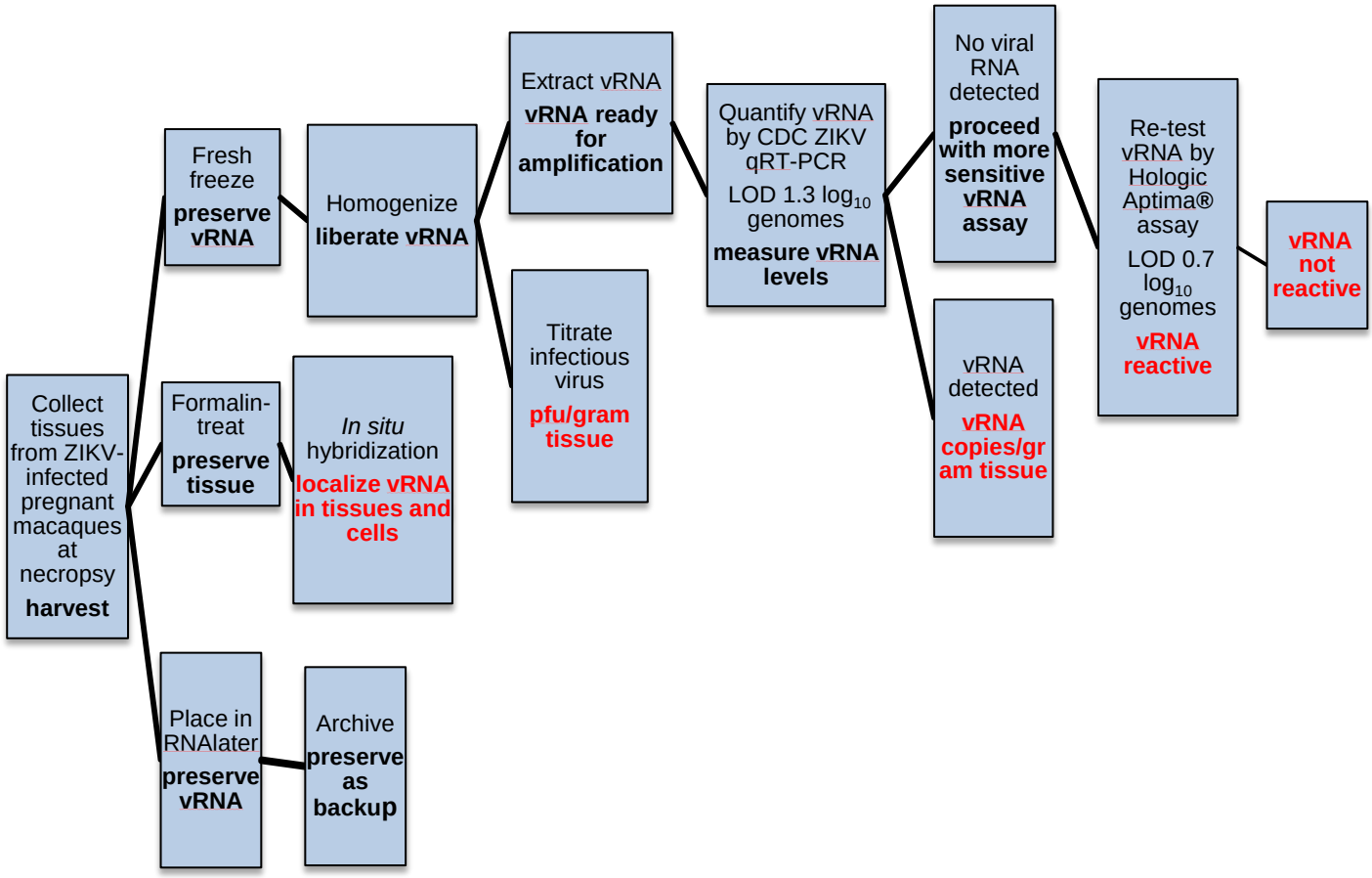

Figure 1: Workflow for detecting ZIKV in tissues. vRNA: Zika virus RNA, LOD: limit of detection, pfu: plaque forming units

vRNA isolation from tissues

Tissue samples were placed into 2.0 mL round bottom tubes holding a single 5 mm steel or glass bead and 250 uL Dulbecco's Modified Eagle Medium (DMEM). Tubes were weighed and tissue weights were

determined by subtracting the mass of the tube, bead, and medium without the tissue. Tissues were homogenized for 2 m at 30 shakes/second (s) in a Mixer Mill (Qiagen). The homogenate was centrifuged for 2 m at 14,000 g to clarify the supernatant. If liquefaction of tissues was incomplete, samples were homogenized for an additional 2 m at 30 shakes/s and if that second step failed to achieve liquefaction, an additional 250 ul of DMEM was added, and the sample was re-homogenized. Many samples required repeated homogenizations, and we observed that several tissues created a thick froth upon homogenization. No sample tested required more than 750 uL total of DMEM to yield the requisite 140 uL of liquefied sample. The total volume of media added to each sample was recorded, and used to normalize the final RNA concentration results after qRT-PCR. Our previous experiments using tissues spiked with known RNA copy numbers of ZIKV (12) revealed that homogenization resulted in a mean loss of 1.7 $\log_{10}$ RNA copies. RNA was extracted from 140 ul of homogenized tissue supernatants using the viral RNA mini kit (Qiagen) according to the manufacturer's instructions with deviations in tissue sample volumes or elution volumes noted and used to adjust the final RNA concentrations. All RNA extracts were eluted in 60 uL of DEPC-treated water for storage at -80°C prior to quantification. Levels of vRNA in samples are expressed as mean $\log_{10}$ RNA copies per gram of tissue or ml.

vRNA quantitation by quantitative real time polymerase chain reaction (qRT-PCR)

Zika virus RNA was measured in triplicate by reverse transcription qRT-PCR on an Applied Biosystems ViiA 7 machine using the Taqman Fast Virus 1-Step Master Mix (Thermo 4444436) and published primers and probe from Lanciotti *et al*. (ZIKV 1086, ZIKV 1162c, and ZIKV 1107-FAM) (14). Briefly, 9.6 uL of extracted viral RNA was used as a template in a total reaction volume of 20 uL. The qRT-PCR machine was programmed for an initial reverse transcription step at 50ºC for 5 minutes, followed by a single denaturation step at 95ºC for 20 seconds. Next, the repeated steps of denaturation at 95ºC for 3 seconds and elongation at 60ºC for 30 seconds for a total of 40 iterations. Each 96-well plate included a standard curve, generated from serial dilutions of the inocula RNA, as well as a no-template control that consisted of DMEM diluent processed alongside the tissue samples. The Brazil 2015 stock strain was quantified relative to a standard curve of the French Polynesia 2013 stock strain. The latter was quantified both by a computational method based on maximum-likelihood estimation for copy, and also relative to a quantified virus standard obtained from the European Virus Archive (Zika standard #1, H/PF/2013 inactivated). Both quantitation methods yielded the same copy number value for the French Polynesia 2013 stock strain. The limit of detection varied depending on the weight of tissue sampled and volume of DMEM needed to homogenize to liquefaction, with a mean of 2.3 (range 1.4-4) $\log_{10}$ RNA copies. For all samples that lacked detectable ZIKV RNA by the qRT-PCR assay, the Hologic Aptima® ZIKV assay was used on the remaining 0.2-1.0 ml volume of plasma or tissue homogenate (see Appendix: Aptima dilutions). Aptima® is a qualitative *in vitro* assay that detects vRNA on a fully automated Panther® system and is currently approved by the FDA for clinical use under an Emergency Use Authorization (15). A buffer solution was added to tissue homogenates tested by the Aptima® assay to achieve a total volume of 1.3 ml, where the maximum dilution on 0.2 ul homogenates was 6.5X; most samples only required dilutions of 2-3X. All steps were performed in one tube with an internal control and a limit of detection of 0.7 $\log_{10}$ RNA copies/ml.

Viral quantification by plaque assay

Vero cells starting at passage 5 from the American Type Culture Collection were used for virus titrations by plaque assay. Confluent 6- or 12-well Vero plates were inoculated with 250 or 125 µl, respectively, of ten-fold dilutions of macaque plasma, cerebral spinal fluid, urine, or tissue homogenates in MEM supplemented with 10% fetal bovine serum and allowed to absorb at 37°C for 1 h. When plasma samples were viscous and clumped undiluted, the first dilution tested was 1:10. After incubation, each cell monolayer was overlaid with 2 (12-well plates) or 4 ml (6-well plates) 0.8% agar (liquefied 10% agar, ultrapure agarose [Invitrogen] diluted in 42°C MEM) and allowed to solidify. The plates were incubated at 37°C for 8 days. Cell

monolayers were then fixed with 4% formalin for 30 min, agar plugs were removed, and 0.025% gentian violet (Sigma) in 30% ethanol was overlaid in each well to stain viable cells. Viral titers were recorded as the reciprocal of the highest dilution where plaques are noted. The limit of detection of the assay for 6-well plates was 1.6 $\log_{10}$ PFU/ml and 1.9 $\log_{10}$ PFU/ml for 12-well plates.

Histopathological analyses using hemotoxylin and eosin

Macaque tissues were placed in 10% buffered formalin with standard processing and then paraffin embedded, sectioned, and hematoxylin and eosin stained. All tissues were evaluated microscopically by an American College of Veterinary Pathologists-boarded veterinary anatomic pathologist with expertise in non-human primates. Each tissue was evaluated without knowledge of the viral status of that particular tissue.

Histopathological analyses using *in situ* hybridization: For in situ hybridization (ISH), probes were designed to hybridize to the positive sense ZIKV RNA genome. One set ('ZIKV') was designed to detect both African and Asian ZIKV strains (AY632535.2; KU321639.1), and it consists of 80 paired probes spanning the region from 139 to 4697 in a ZIKV reference genome (NC_012532.1). A second probe set ('ZIKV-2015') that hybridizes perfectly (0 mismatches) to the Brazil_SPH2015 strain used to inoculate macaques consists of 70 paired probes covering genomic nucleotides 150 to 4168. A positive riboprobe control for DNA integrity in the tissue sections was a probe recognizing ubiquitin C (Mm-Ubc-O1 Cat No. 484311) and a negative control riboprobe detects bacterial dihydrodipicolinate reductase (DapB-C2, Cat No. 310043-C2). Chromogenic *in situ* hybridization was carried out according to the manufacturer's instructions for nucleic acid detection (RNAscope 2.5 Brown Kit). Formalin fixed paraffin embedded slides were baked at 60°C for 1 hour, then deparaffinized with exposure to xylene twice, 10 minutes each time, followed by stirring in 100% ethanol twice and air-drying, then rehydration with ddH2O for 2 minutes. Hydrogen peroxide, supplied by the manufacturer (Pretreatment 1) was applied to the slides for 10 minutes at room temperature. The slides were then boiled in "Pretreatment solution 2", at 100°C for 15 minutes, followed by protease digestion in "Pretreatment solution 3" for 30 minutes at 40°C to allow target accessibility. Zika-genome specific or control probes were applied and the slides were incubated at 40°C for 2 hours. Slides were washed twice with 1X wash buffer for 2 min at room temperature. A series of six signal amplification steps were performed per manufacturer's instructions. Incubation with DAB solution was performed at room temperature and the reaction was quenched with dH2O. Slides were counterstained with Gill's Hematoxylin. Slides were passed through 100% ethanol, 70% ethanol, and twice in xylene before coverslipping with xylene based mounting medium. Slides were counterstained with hematoxylin and mounted with xylene-based SHUR/Mount (Triangle Biomedical Sciences). Positive staining was identified as brown, punctate dots. Slides were digitized using an Olympus VS120 scanner and a 40X objective with bright field illumination.

Results

Clinical Outcomes

Macaques were observed at least twice daily for clinical signs of disease including inappetence, stool quality, dehydration, diarrhea, and lethargy. Rectal temperature was collected at every sedation. No clinical signs, including fever, lethargy, weight loss, or skin rash were observed in any of the dams. For the dam inoculated at GD41, ultrasounds did not detect any fetal abnormality 2 days post-inoculation (dpi) at amniocentesis, or 3 and 5 dpi (no amniocentesis), but at 7 dpi the fetal heartbeat was absent. In response, the animal was euthanized for necropsy and collection of maternal and fetal tissues. No bacteria could be isolated from amniotic fluid collected at necropsy, suggesting that iatrogenic bacterial infection through the amniocentesis procedures was unlikely the cause of fetal death. The dam that was ZIKV inoculated on GD65 had intermittent vaginal bleeding starting at GD103, and birthed an abnormally small (282 grams) but

viable neonate on GD151, i.e. 87 dpi. The neonate had a smaller biparietal diameter and head length compared to mock-inoculated GD-matched fetuses or colony age-matched controls (data not shown), but the biparietal/femur length ratio (as a measure of relative head size to total body size) was within the range of control animals, suggesting that the smaller head measurements were a reflection of overall stunted body growth (data in preparation for publication). The dams inoculated at GD50 and GD90 were euthanized prior to delivery on GD155, i.e. 105 and 65 dpi, respectively, 10 days pre-term. Their fetuses showed no gross differences in body or head size compared to same-aged CNPRC colony averages.

Sample Collections

Unfortunately, since death of the GD41 inoculated fetus was unexpected, the emergency necropsy only allowed collection of 11 tissues. Umbilical cord blood was not obtained from the GD65 neonate that birthed prematurely. Samples from the other 3 study animals were unfortunately not testable. The bronchial lymph nodes were not collected from the GD50 inoculated dam. Amniotic fluid was not sampled from the GD65 animal that birthed prematurely. For all of the other tissue samples in the study, samples were successfully obtained and archived as in the methods. All animals had cleared detectable plasma ZIKV RNA levels at necropsy (data not shown). The dam inoculated at GD90 developed a recrudescent ZIKV RNA in plasma 43 dpi, but contained no detectable RNA in her plasma by necropsy, 65 dpi (data not shown.)

Tissue distribution of ZIKV RNA in pregnant macaque tissues is diffuse and persists long after infection. ZIKV RNA was detected in selected pregnant macaque tissues 7, 65, 87, or 105 dpi. None of the pregnant animals contained detectable ZIKV RNA by qRT-PCR at necropsy, indicating no possibility of tissue contamination by blood. However, 20-92% of tissues sampled from each animal contained detectable ZIKV RNA by qRT-PCR or Aptima® at necropsy (Table 2).
Furthermore, 43-66% of the tissues that did not contain detectable ZIKV RNA by the qRT-PCR were determined to be ZIKV RNA reactive by the qualitative Aptima® assay (Table 3), confirming that the Lanciotti qRT-PCR is not as sensitive as Aptima®. Most of the tissues that tested ZIKV RNA negative by the qRT-PCR but that were Aptima® assay reactive were in the lymphoid system (Table 4). ZIKV RNA positive tissues assayed by both RNA detection methods and in all 4 dams were lymphatic and genitourinary tissues, suggesting these are the primary targets (Table 4, Figure 2).

Table 2: ZIKV RNA and infection rates in tissues from 4 experimentally infected pregnant rhesus macaques

Macaque identifier	**118	**723	**924	**449
Gestation day at inoculation	41	50	64	90
Gestation day at necropsy	48	155	151	155
Days post-inoculation at time of necropsy	7	105	87	65
% of tissues containing ZIKV RNA	92% (11/12)	31% (11/36)	25% (9/35)	33% (12/36)
% of ZIKV RNA positive tissues containing infectious ZIKV	27% (3/11)	9% (1/11)	11% (1/9)	0% (0/12)

Table 3: Sensitivity of ZIKV qRT-PCR versus Aptima® assay for vRNA detection

Macaque identifier	**118	**723	**924	**449
Number of qRT-PCR vRNA positive tissues	11	4	2	3
Number of Aptima® vRNA positive tissues	nt	7	5	9
Sensitivity of qRT-PCR	nt	57%	40%	33%

Some dams also contained detectable ZIKV RNA in cardiopulmonary, integument, musculoskeletal, and digestive tissues. The dam inoculated 7 days before necropsy had both highest rate of ZIKV RNA tissue positivity as well as the highest ZIKV RNA levels, ranging from 1.8 $\log_{10}$ genomes/ml or gram tissue in the kidney to 10.4 in the amniotic fluid (Table 4, Figure 2A).

Table 4: ZIKV RNA and infectious virus in experimentally inoculated macaque tissues**:**														
System	**Tissue**	****118**			****723**			****924**			****449**			**animal #**
		41			**50**			**64**			**90**			**GD at inoc.**
		48			**155**			**151**			**155**			**GD at necrop.**
		7			**105**			**87**			**65**			**necropsy dpi**
		log10 genome/g or ml	**Holagic RNA**	**log10 PFU/ml or gram**	**log10 genome/g or ml**	**Holagic RNA**	**log10 PFU/ml or gram**	**log10 genome/g or ml**	**Holagic RNA**	**log10 PFU/ml or gram**	**log10 genome/g or ml**	**Holagic RNA**	**log10 PFU/ml or gram**	
Lymphoid	Retropharyngeal lymph node	nc	nc	nc	nr	**R**	nt	nr	nr	nt	nr	**R**	nt	
	Inguinal lymph node	**6.4**	nt	<420	**5.1**	nt	neg	**5.3**	nt	neg	**6.4**	nt	neg	
	Cervical lymph node	nc	nc	nc	nr	**R**	nt	nr	**R**	nt	nr	**R**	nt	
	Peri-aortic lymph node	nc	nc	nc	nr	**R**	nt	**3.7**	nt	neg	**5.2**	nt	neg	
	Bone Marrow	**2.4**	nt	<213	nr	**R**	nt	nr	**R**	nt	nr	**R**	nt	
	Bronchial lymph nodes	nc	nc	nc	nc	nc	nc	nr	nr	nt	nr	**R**	nt	
Cardiopulmonary	Pulmonary artery, L +R	nc	nc	nc	nr	nr	nt	nr	nr	nt	nr	nr	nt	
	Heart, atrio-ventricular valves	**6.1**	nt	neg	nr	nr	nt	nr	nr	nt	nr	nr	nt	
	Pericardium	nc	nc	nc	nr	nr	nt	nr	nr	nt	nr	nr	nt	
	Aortic valve	nc	nc	nc	nr	nr	nt	nr	nr	nt	nr	nr	nt	
	Aorta, thorax	nc	nc	nc	nr	nr	nt	nr	**R**	nt	nr	nr	nt	
	Aorta, abdomen	nc	nc	nc	nr	nr	nt	nr	nr	nt	nr	nr	nt	
	Oropharynx	nc	nc	nc	nr	**R**	nt	nr	nr	nt	nr	nr	nt	
	Lung Caudal	**4.2**	nt	<80	nr	nr	nt	nr	nr	nt	nr	nr	nt	
	Bronchi	nc	nc	nc	nr	nr	nt	nr	nr	nt	nr	nr	nt	
Digestive	Liver & gall bladder	nr	nt	nt	nr	nr	nt	nr	nr	nt	nr	**R**	nt	
	Pancreas	nc	nc	nc	nr	nr	nt	nr	nr	nt	nr	nr	nt	
	Duodenum	nc	nc	nc	nr	**R**	nt	nr	nr	nt	nr	nr	nt	
	Jejunum	**4.0**	nt	<440	nr	nr	nt	nr	nr	nt	nr	**R**	nt	
	Ileum	**5.3**	nt	<420	nr	nr	nt	nr	**R**	nt	nr	nr	nt	
Integument	Fat tissue	nc	nc	nc	nr	nr	nt	nr	nr	nt	nr	nr	nt	
	Skin, intrascapular	nc	nc	nc	nr	nr	nt	nr	nr	nt	nr	**R**	nt	
	Skin, medial thigh	nc	nc	nc	nr	nr	nt	nr	nr	nt	nr	nr	nt	
Musculoskeletal	Muscle, quadriceps	nc	nc	nc	nr	nr	nt	nr	nr	nt	nr	nr	nt	
	Cartilage, L knee	nc	nc	nc	nr	nr	nt	nr	nr	nt	nr	nr	nt	
	Tendon/ligaments, L knee	nc	nc	nc	nr	nr	nt	nr	nr	nt	nr	nr	nt	
	Bone	nc	nc	nc	nr	nr	nt	nr	nr	nt	nr	nr	nt	
	Finger, distal 2 cm	nc	nc	nc	nr	nr	nt	nr	**R**	nt	nr	nr	nt	
	Fascia	nc	nc	nc	nr	nr	nt	nr	nr	nt	**2.8**	nt	neg	
Genitourinary	Kidney, L	**1.8**	nt	<80	nr	nr	nt	nr	nr	nt	nr	nr	nt	
	Ovary	**4.8**	nt	<420	nr	**R**	nt	nr	nr	nt	nr	nr	nt	
	Umbilical cord	**8.3**	nt	**6.9**	**3.4**	nt	neg	3.5	nt	neg	nr	nr	nt	
	Placenta	**8.8**	nt	**3.2**	**4.4**	nt	**13***	3.9	nt	**140****	nr	**R**	nt	
	Umbilical cord blood	nc	nc	nc	nc	nc	nc	nc	nc	nc	nc	nc	nc	
	Amniotic fluid	**10.4**	nt	**6.0**	**2.5**	nt	neg	nc	nc	nc	nr	**R**	nt	
Neuroendocrine	Eye cornea, L	nc	nc	nc	nr	nr	nt	nr	nr	nt	nr	nr	nt	
	Eye sclera, L	nc	nc	nc	nr	nr	nt	nr	nr	nt	nr	nr	nt	

Nt: not tested, nc: not collected, **R**: reactive nr: not ZIKV RNA reactive, *full placental thickness, **maternal side of placenta.

Infectious ZIKV in RNA positive macaque tissues was rarely detected. Given our previous work that showed 100-10,000 times more ZIKV RNA copies than PFU in the same sample (12), coupled with the limit of detection of the plaque assay, which varied according to the volume of solid tissue sampled, but averaged 2.4 $\log_{10}$ PFU per gram of tissue, we did not attempt plaque assays on samples that contained less than <3 $\log_{10}$ genome. Despite detection of ZIKV RNA at high levels in a significant number of tissues from all 4 animals, only 3/11 (27%) of tissues from the GD41 animal contained infectious virus above the limit of detection. The 3 tissues were the placenta that had 3.2 $\log_{10}$ PFU/gram, the amniotic fluid that contained 6.0 and the umbilical cord that contained 6.9. The only other tissue that contained infectious virus were the placentas from the GD50 and GD64 inoculated dams that contained 1.1 and 2.1 $\log_{10}$ PFU/gram, respectively.

Histopathologic analyses. The majority of the histopathologic changes observed in all 4 dams are commonly seen in adult rhesus macaques indicating that they are likely are nonspecific and incidental. Dam **118 that had fetal death at 7 dpi had a mild fibrinonecrotizing placentitis (Figure 3) that may be linked to ZIKV infection. Bacterial cultures on the amniotic fluid were negative, and no signs of bacterial placentitis were observed. The neutrophilic placentitis and omphalophlebitis in the GD64 inoculated dam were likely due to an ascending bacterial infection, as bacteria were seen within the lesions histologically. This animal also had mild pulmonary edema, likely secondary to the bacterial infection. The hepatic nodular regeneration, fibrosis and cholecystitis in the GD50 inoculated dam is not a common lesion seen in macaques, and the exact cause is unknown, however, it is highly unlikely to be related to ZIKV infection, because it is chronic and not inflammatory. Other notable histopathologic changes in tissues included in this study are detailed in Table 6.

***In situ* hybridization.** *In situ* hybridization (ISH) probes for ZIKV and control probes were designed and used. Most tissues that contained ZIKV RNA by qRT-PCR or Aptima® assays were used for tissue and cell specific hybridization analysis. ZIKV-positive tissues from non-pregnant ZIKV-inoculated macaques in another study were used as positive controls. Two negative controls were 1) nucleotide matched-scrambled probes on serial sections and 2) selected tissues from non-infected animals and from the placebo-inoculated macaques in this study that were not ZIKV RNA reactive. No ISH reactivity was observed in negative controls. ISH reactivity was verified by at least duplicate assays. ISH confirmed the presence of ZIKV RNA in most tissues that contained RNA detected by qRT-PCR and Aptima® (Table 5), where the highest concordance between RNA reactivity by qRT-PCR and Aptima and ISH was in the dams inoculated at GD60 and GD90. There was not a clear correlation between the ZIKV copy number by qRT-PCR and the magnitude of ISH reactivity, although the latter technique is semi-quantitative. Most lymph nodes contained ISH detectable RNA in individual trafficking cells (sinusoidal, presumed macrophages) (Figures 4 and 5) and/or within multiple germinal centers (dendritic cells) (Figure 6). In the uterus, kidney, gall bladder, and ileum, rare individual epithelial lining cells contained ZIKV RNA detected by ISH (data not shown).

Table 5: Tissues from ZIKV inoculated macaques RNA reactive by qRT-PCR and Aptima or *in situ* hybridization

Animal number	GD at inoculation	GD at necropsy	Days post-inoculation	RNA reactive by qRT-PCR or Aptima	ISH positive/ISH tested (%)
**118	41	48	7	11	3/8 (38%)
**723	50	155	105	11	5/9 (56%)
**924	64	151	87	7	7/7 (100%)
**449	90	155	65	10	6/7 (86%)

Table 6: Histopathologic changes in rhesus macaques inoculated with Zika virus						
System	**Tissue**	**118	**723	**924	*449	**animal #**
		41	50	64	90	**inoculation (GD)**
		48	155	151	155	**necropsy (GD)**
		7	105	87	65	**necropsy dpi**
Lymphoid	Retropharyngeal lymph node	nc	Mild lymphoid hyperplasia	Moderate lymphoid hyperplasia	Mild lymphoid hyperplasia	
	Inguinal lymph node	Mild medullary plasmacytosis	WNL	Moderate lymphoid hyperplasia	Mild lymphoid hyperplasia	
	Cervical lymph node	nc	WNL	Mild lymphoid hyperplasia	Mild lymphoid hyperplasia	
	Peri-aortic lymph node	nc	WNL	WNL	WNL	
	Bone marrow	WNL	Insufficient sample	WNL	WNL	
	Bronchial lymph nodes	nc	nc	Moderate lymphoid hyperplasia	Moderate medullary histiocytosis (pneumoconiosis)	
Cardiopulmonary	Pulmonary artery, L +R	nc	ne	ne	ne	
	Heart, R and L, atrio ventricular valves	Rare myocardial lymphocytic infiltrates	WNL	WNL	WNL	
	Pericardium	nc	ne	ne	ne	
	Aortic valve	nc	ne	ne	ne	
	Aorta, thorax	nc	WNL	WNL	WNL	
	Aorta, abdomen	nc	ne	ne	ne	
	Oropharynx	Tonsil: Mild lymphoid hyperplasia	nc: Tonsil: moderate lymphoid hyperplasia; other structures: WNL	nc	WNL (no lymphoid tissue)	
	Lung, caudal	WNL	WNL	Mild pulmonary edema	Mild pneumoconiosis	
	Bronchi	nc	ne	ne	ne	
Digestive	Liver, left lateral lobe (include gall bladder)	Rare clusters of macrophages and neutrophils with shrunken hepatocytes	Nodular hyperplasia with bridging fibrosis; moderate zonal hepatocellular vacuolation (lipidosis and glycogenosis); moderate chronic lymphoplasmacytic cholecystitis	Diffuse moderate glycogenosis	Mild periportal lymphoplasmacytic hepatitis; mild lymphoplasmacytic cholecystitis	
	Pancreas	nc	ne	ne	ne	
	Duodenum	nc	WNL	WNL	WNL	
	Jejunum	WNL	WNL	WNL	WNL	
	Ileum	WNL	WNL	WNL	WNL	
			ne			
Integument	Fat tissue	nc	ne	ne	ne	
	Skin, shaved, dermis and epidermis, intrascapular	nc	WNL	WNL	WNL	
	Skin, shaved, dermis and epidermis, medial thigh	nc	ne	ne	ne	
			ne			
Musculoskeletal	Muscle, quadriceps	nc	ne	ne	ne	
	Cartilage, L knee	nc	ne	ne	ne	
	Tendon/ligaments, L knee	nc	ne	ne	ne	
	Bone	nc	ne	ne	ne	
	Finger, distal 2 cm	nc	nc	nc	nc	
	Fascia	nc	nc	nc	nc	
Genitourinary	Kidney, L	Mild, perivascular lymphocytic infiltrates; mild medullary amyloidosis	Mild, perivascular lymphocytic infiltrates	Mild, perivascular lymphocytic infiltrates	Mild, perivascular lymphocytic infiltrates	
	Ovary	WNL	WNL	WNL	WNL	
	Umbilical cord	WNL	WNL	Neutrophilic omphalophlebitis	WNL	
	Placenta	Mild fibrinous and necrotizing placentitis	WNL	Neutrophilic placentitis	WNL	
	Umbilical cord blood	n/a	n/a	n/a	n/a	
	Amniotic fluid at necropsy	n/a	n/a	n/a	n/a	
Neuroendocrine	Dura Mater	nc	ne	ne	ne	
	Eye cornea, L	nc	ne	ne	ne	
	Eye sclera, L	nc	ne	ne	ne	

WNL: within normal limits, nc: not collected, ne: not examined, n/a: not applicable

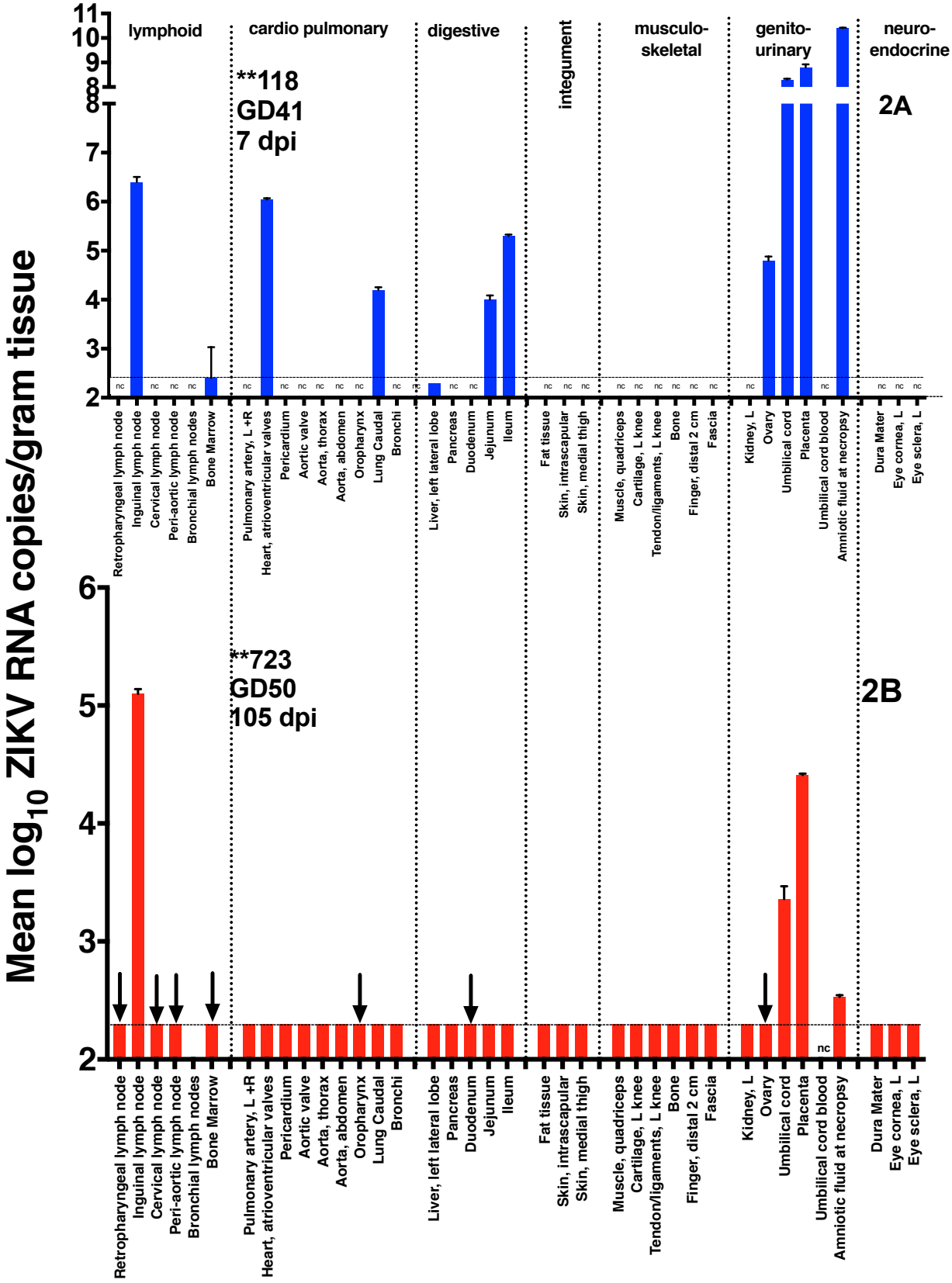

Figure 2: ZIKV RNA copies in tissues of pregnant rhesus macaques **(A)** inoculated at GD41 and harvested at 7 dpi and **(B)** GD50 and 105 dpi. nc is not collected. Samples that did not contain detectable RNA by the qRT-PCR are recorded at the limit of detection, 2.3 log 10 RNA copies/gram. Black arrows show tissues that tested reactive by the Hologic Aptima® assay. Error bars show standard deviations for 3 RNA measurements per sample.

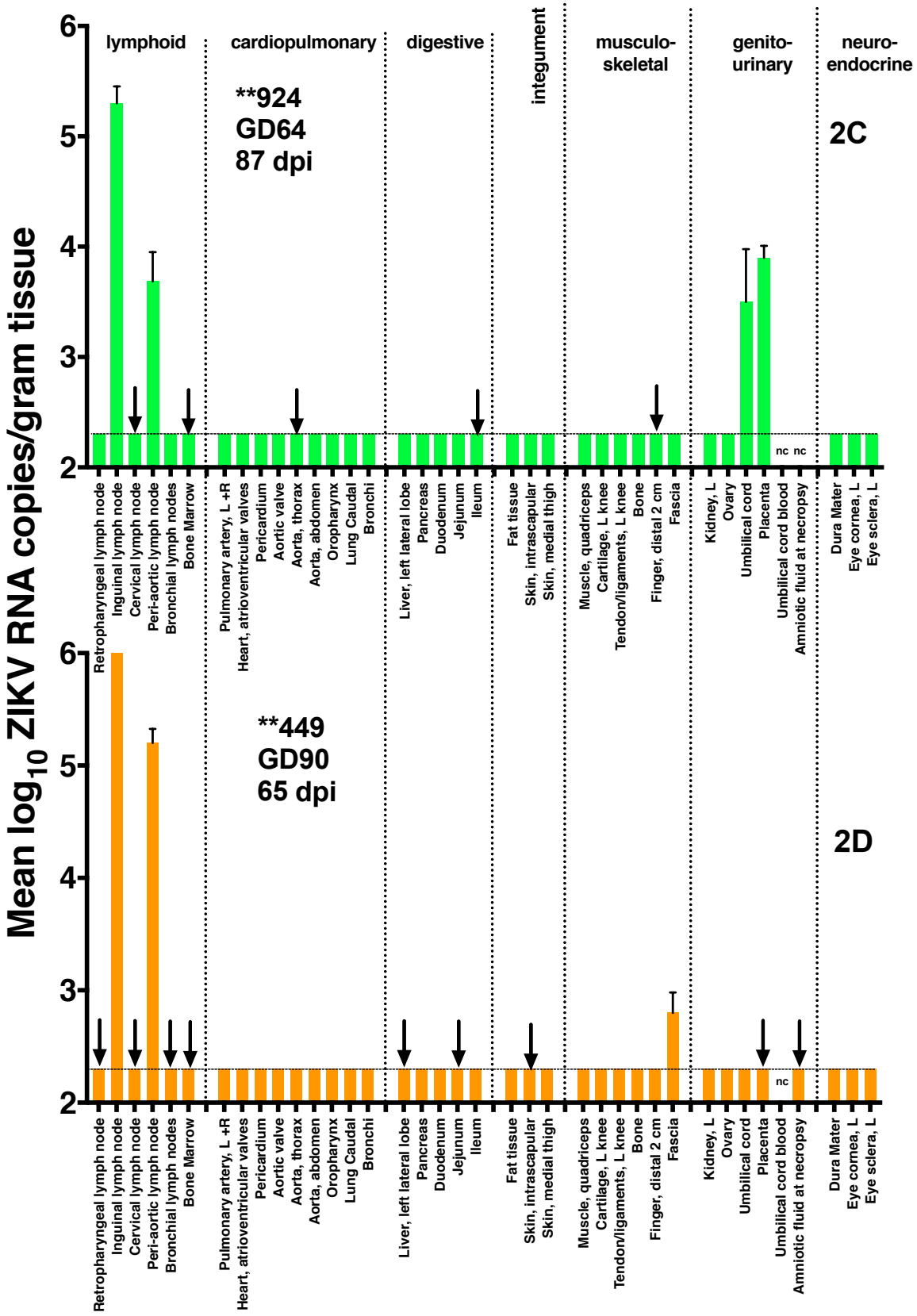

Figure 2: ZIKV RNA copies in tissues of rhesus macaques **(C)** inoculated at GD64 and harvested at 87 dpi, and **(D)** GD60 and 65 dpi. nc is not collected. Samples that did not contain detectable RNA by the qRT-PCR are recorded at the limit of detection, 2.3 log 10 RNA copies/gram. Black arrows show tissues that tested reactive by the Hologic Aptima® assay. Error bars show standard deviations for 3 RNA measurements per sample.

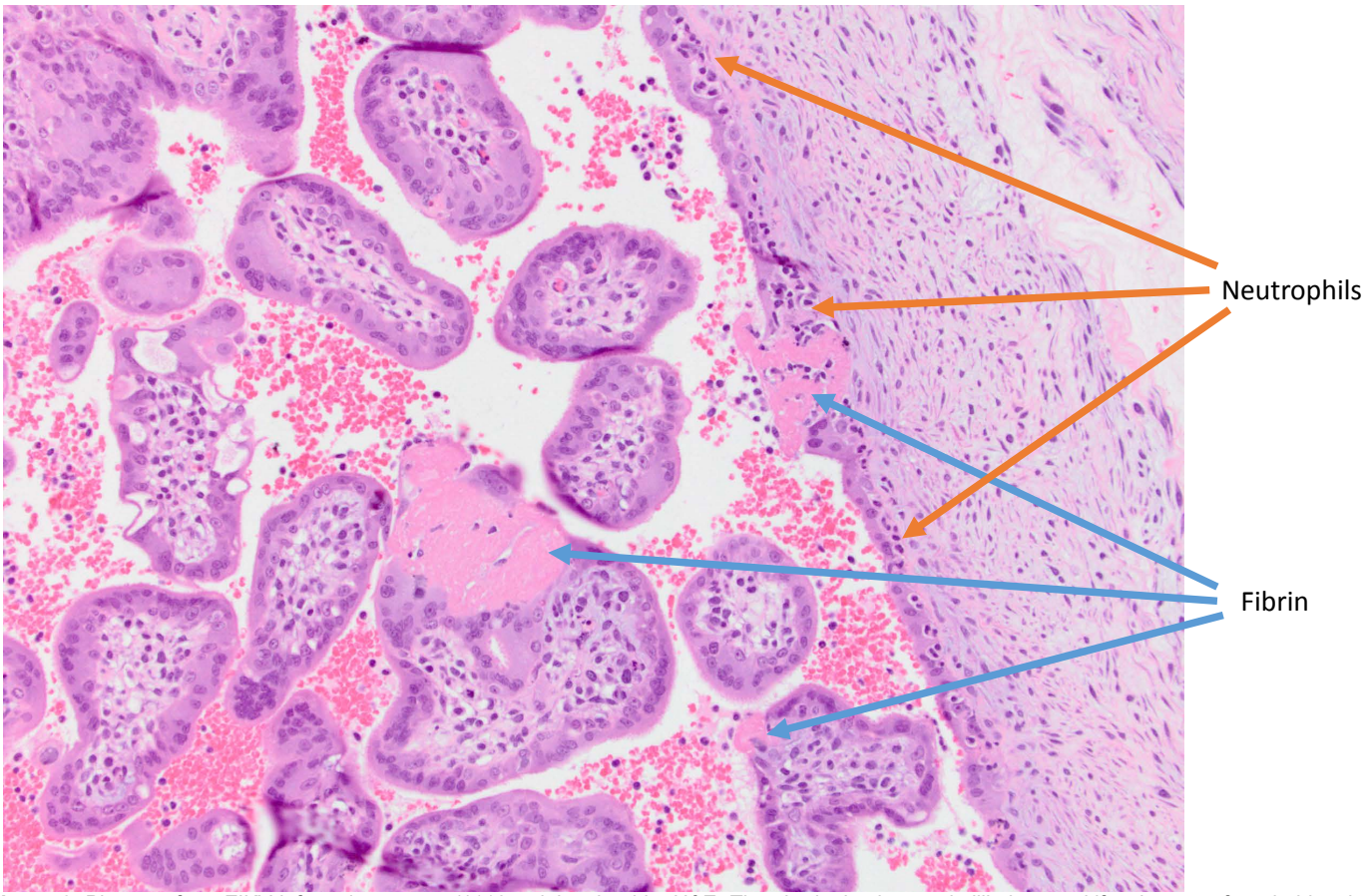

Figure 3: Placenta from ZIKV-infected macaque **118 7 dpi stained by H&E. The chorionic plate and villi show multifocal areas of trophoblast loss that are replaced by fibrin (blue arrows) and small numbers of neutrophils (orange arrows). Additionally, there are small numbers of neutrophils (orange arrows) within the trophoblastic lining of the chorionic plate.

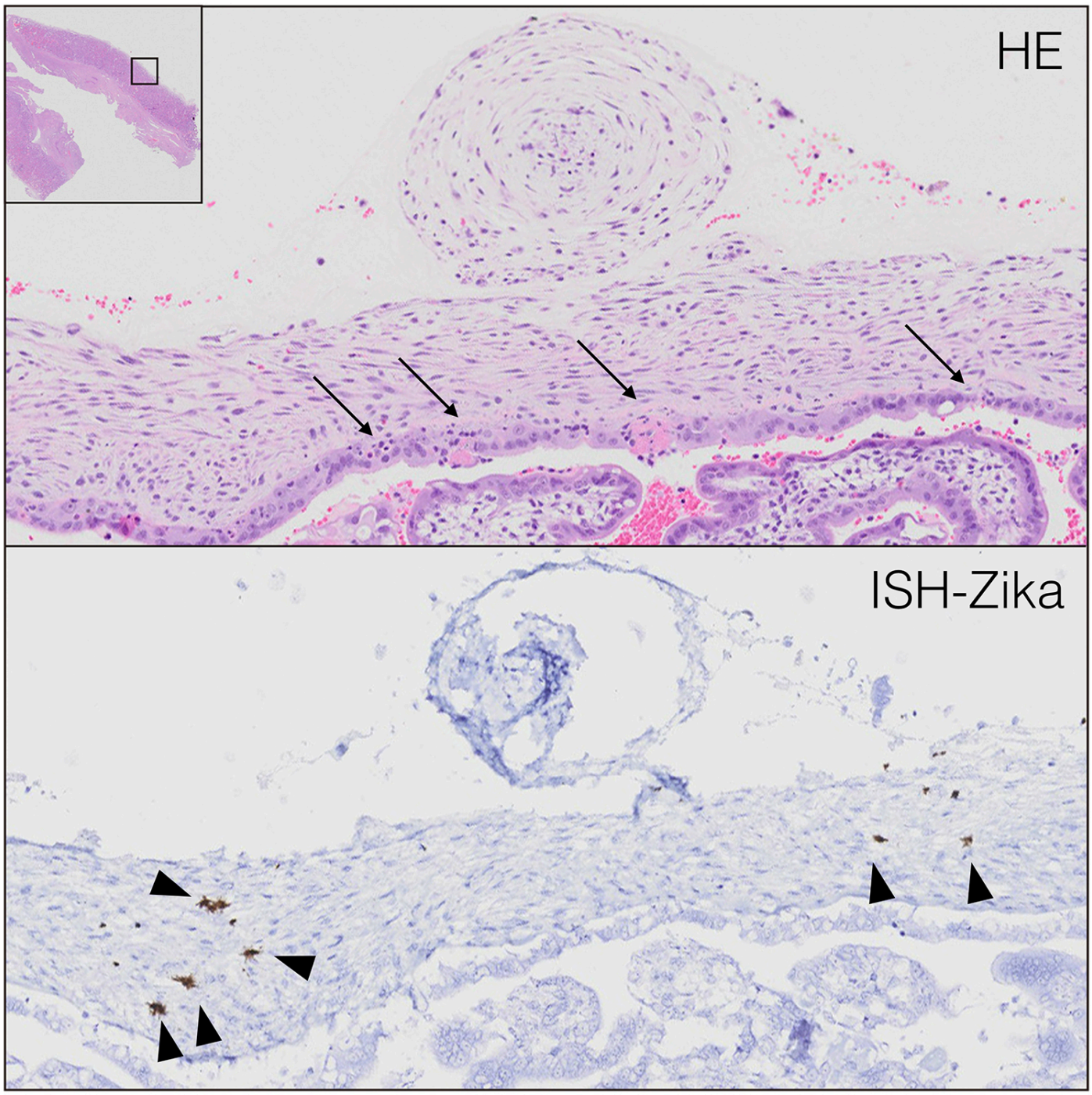

Figure 4: Placenta from ZIKV-infected macaque **118 7 dpi stained by H&E (upper) and ISH (lower). ZIKV RNA (arrowheads) is detectable within cells of the chorionic plate, near regions of fibrinous placentitis (arrows). The inset shows an overview of the tissue location.

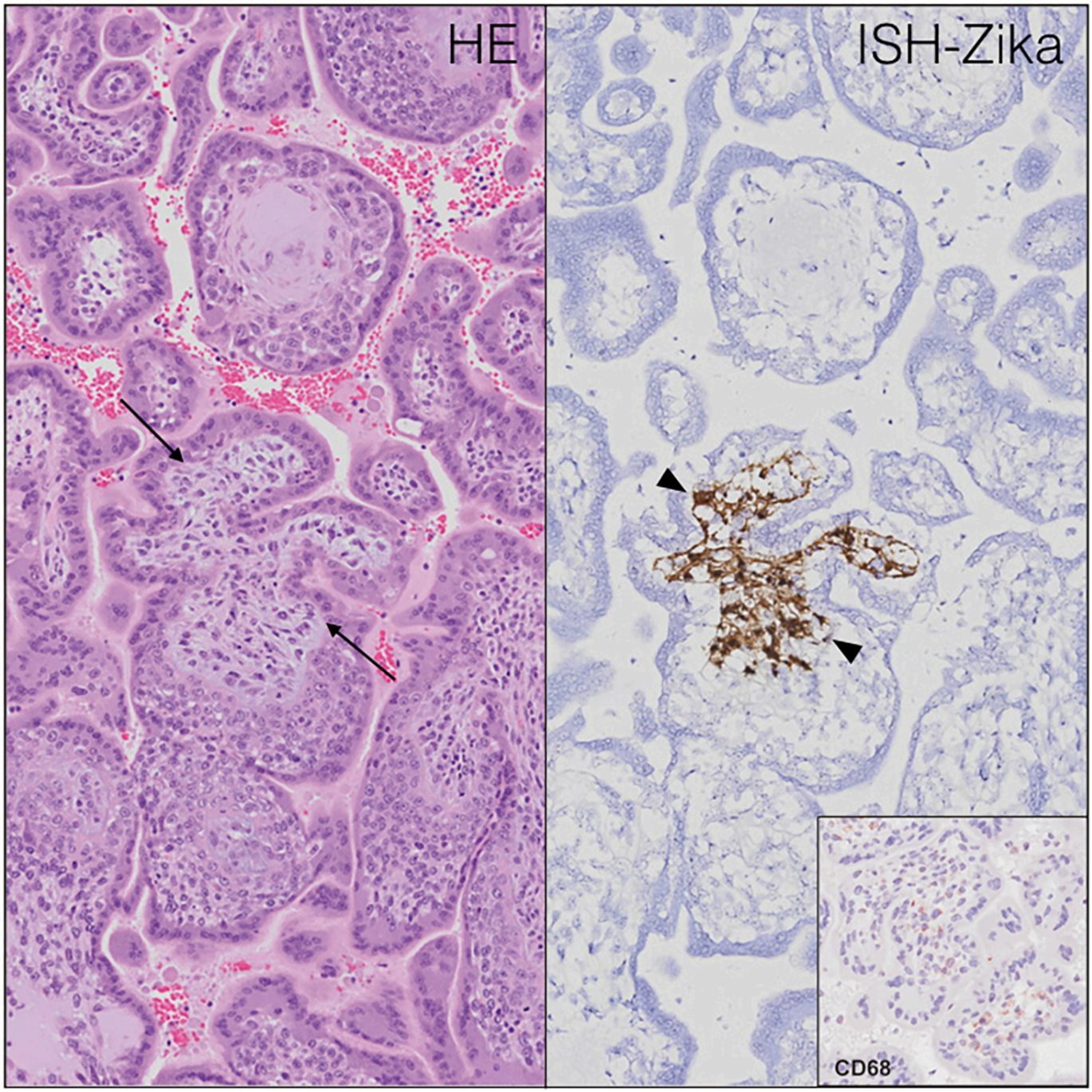

Figure 5: Placenta from ZIKV-infected macaque **118 7 dpi stained by H&E (left) and ISH (right). Chorionic villi contain normal stromal cells, which include placental macrophages (HE, arrows). Macrophages (CD68 positive) within inflamed chorionic villi contained ZIKV RNA.

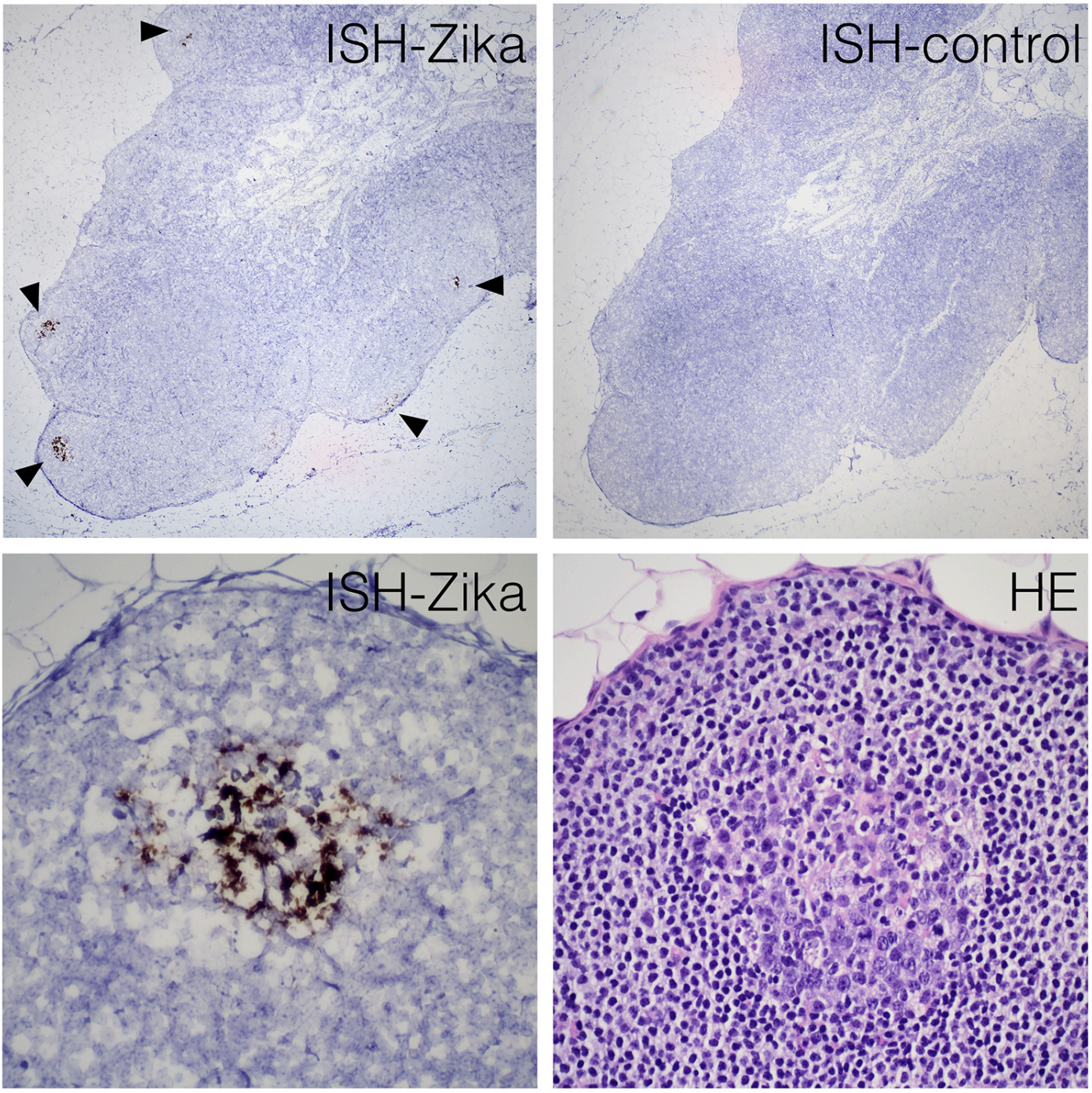

Figure 6: Inguinal lymph node showing ZIKV RNA in over half of the germinal centers (arrowheads) of the section of node pictured. Using a scrambled, nucleotide-matched control, there is no detectable signal. Hybridization is strongest in the dendritic cell-rich germinal centers.

Summary

The results from this study reveal that detectable ZIKV RNA persists in selected tissues from pregnant rhesus macaques intravenously and intraamniotically inoculated with a 2015 strain of ZIKV from Brazil.

Zika virus RNA was detected in tissues from all 4 animals in this study. Persistence of ZIKV RNA was detected for up to 105 days, the latest time tissues were sampled post-inoculation. The dam sampled 7 dpi had the greatest proportion of ZIKV RNA positive tissues, the highest ZIKV RNA levels and were more likely to contain infectious ZIKV compared to the other 3 dams in the study sampled, at 65, 87, or 105 days after inoculation. In all 4 animals, ZIKV RNA was detected in lymphatic and genitourinary tissues. Some animals also contained detectable ZIKV RNA in cardiopulmonary, digestive, and musculoskeletal tissues. The qualitative Aptima® assay from Hologic showed ZIKV reactivity in up to 60% of tissues that were RNA negative by the conventional qRT-PCR, revealing its increased sensitivity.

Infectious ZIKV was detected in placental samples from 3 of the dams, the umbilical cord (1 animal), and amniotic fluid (1 animal). The peak infectious titer of 6.9 $\log_{10}$ PFU/ml was detected in the umbilical cord of the animal inoculated at GD41 and collected 7 dpi. The absence of infectious ZIKV in all other tissues tested can be interpreted in several ways: 1) those tissues truly lack infectious ZIKV, 2) infectious ZIKV is present at levels below the 1.9 $\log_{10}$ PFU/gram limit of detection of our assays, or 3) the distribution of infectious ZIKV in infected tissues is not uniform, and we by chance sampled fragments in infectious tissues that lacked infectious virus.

Histopathological analyses showed changes commonly seen in adult rhesus macaques, indicating that they are likely are nonspecific and incidental. ZIKV RNA detected in tissues that showed no histopathological changes indicates that the presence of viral RNA is not always associated with lesions. A positive *in situ* hybridization signal that labels ZIKV RNA in cells correlated with ZIKV RNA detected by qRT-PCR and Aptima® in the same tissues in the dams inoculated GD64 and GD90; the correlation was less strong in the dams inoculated at GD41 and GD50. Lymph nodes showed high ISH reactivity including in multiple germinal centers for 3 of 4 lymph nodes from the GD90 macaque and were reactive to a lesser extent in the GD50 and GD64 animals.

Defining the tropism and duration of infectious ZIKV and ZIKV RNA in tissues from rhesus macaques increases understanding of the risk of ZIKV transmission through infected tissue products.

References

1. Centers for Disease Control. Zika virus 2017 [Available from: https://www.cdc.gov/zika/.

2. Rasmussen SA, Jamieson DJ, Honein MA, Petersen LR. Zika Virus and Birth Defects--Reviewing the Evidence for Causality. N Engl J Med. 2016;374(20):1981-7.

3. Pettersson JH, Eldholm V, Seligman SJ, Lundkvist A, Falconar AK, Gaunt MW, et al. How Did Zika Virus Emerge in the Pacific Islands and Latin America? MBio. 2016;7(5).

4. Nelson B, Morrison S, Joseph H, Wojno A, Lash RR, Haber Y, et al. Travel Volume to the United States from Countries and U.S. Territories with Local Zika Virus Transmission. PLoS Curr. 2016;8.

5. Stettler K, Beltramello M, Espinosa DA, Graham V, Cassotta A, Bianchi S, et al. Specificity, cross-reactivity, and function of antibodies elicited by Zika virus infection. Science. 2016;353(6301):823-6.

6. Kawiecki AB, Christofferson RC. Zika-induced antibody response enhances dengue serotype 2 replication in vitro. J Infect Dis. 2016.

7. Dejnirattisai W, Supasa P, Wongwiwat W, Rouvinski A, Barba-Spaeth G, Duangchinda T, et al. Dengue virus sero-cross-reactivity drives antibody-dependent enhancement of infection with zika virus. Nat Immunol. 2016;17(9):1102-8.

8. Kraemer MU, Sinka ME, Duda KA, Mylne A, Shearer FM, Brady OJ, et al. The global compendium of Aedes aegypti and Ae. albopictus occurrence. Sci Data. 2015;2:150035.

9. Bhatnagar J, Rabeneck DB, Martines RB, Reagan-Steiner S, Ermias Y, Estetter LB, et al. Zika virus RNA Replication and Persistence in Brain and Placental Tissue. Emerg Infect Dis. 2017;23(3):405-14.

10. Martines RB, Bhatnagar J, de Oliveira Ramos AM, Davi HP, Iglezias SD, Kanamura CT, et al. Pathology of congenital Zika syndrome in Brazil: a case series. Lancet. 2016;388(10047):898-904.

11. Paz-Bailey G, Rosenberg ES, Doyle K, Munoz-Jordan J, Santiago GA, Klein L, et al. Persistence of Zika Virus in Body Fluids - Preliminary Report. N Engl J Med. 2017.

12. Coffey LL, Pesavento PA, Keesler RI, Singapuri A, Watanabe J, Watanabe R, et al. Zika Virus Tissue and Blood Compartmentalization in Acute Infection of Rhesus Macaques. PLoS One. 2017;12(1):e0171148.

13. Dudley DM, Aliota MT, Mohr EL, Weiler AM, Lehrer-Brey G, Weisgrau KL, et al. A rhesus macaque model of Asian-lineage Zika virus infection. Nat Commun. 2016;7:12204.

14.Lanciotti RS, Kosoy OL, Laven JJ, Velez JO, Lambert AJ, Johnson AJ, et al. Genetic and serologic properties of Zika virus associated with an epidemic, Yap State, Micronesia, 2007. Emerg Infect Dis. 2008;14(8):1232-9.

15. Food and Drug Administration 2017 [Available from: https://www.fda.gov/MedicalDevices/Safety/EmergencySituations/ucm161496.htm - zika.